

Determination of Molecular Orientations in Cubic ND_4NO_3 by Multipole Analysis

BY M. AHTEE AND K. KURKI-SUONIO

Department of Physics, University of Helsinki, Siltavuorenpenger 20 D, 00170 Helsinki 17, Finland

B. W. LUCAS

Department of Physics, University of Queensland, Brisbane, Australia

AND A. W. HEWAT

Institut Laue–Langevin, Grenoble, France

(Received 2 October 1978; accepted 9 January 1979)

Abstract

Rietveld's profile refinement method applied to the neutron powder diffraction data of cubic ND_4NO_3 cannot distinguish between the two best orientation models put forward by Shinnaka [*J. Phys. Soc. Jpn* (1959), **14**, 1073–1083] for rigid NO_3^- . The direct multipole analysis of the nuclear smearing functions yields a model with the values $B_+ = 11.5$ and $B_- = 14.3 \text{ \AA}^2$ for the molecular Debye–Waller factors and 0.99 and 1.23 \AA for the N–D and N–O bond lengths with additional fourth-order multipolar coefficients to describe the deviations from molecular free-rotation. The fourth-order multipolar components are significant. They support the two equivalent orientations model for rigid ND_4^+ tetrahedra with librational amplitude $\langle \theta^2 \rangle^{1/2} = 13.0^\circ$. While the fourth-order multipolar coefficient of NO_3^- represents well the experimental information, its value cannot be explained by any rigid model for NO_3^- but only by an octahedral statistical coordination. This rules out the eight-orientations model and gives a slight preference to the twelve-orientations model.

1. Introduction

This work is part of a project started recently to study the different phases of deuterated ammonium nitrate with neutron powder diffraction. Even though ammonium nitrate has been studied extensively, the only neutron diffraction experiment so far is the determination of the room temperature structure by Choi, Mapes & Prince (1972). However, neutron studies enable us to locate hydrogen atoms more accurately than in X-ray studies.

This report deals with the structural details of the high-temperature cubic phase with CsCl structure

existing between 398 and 442.5 K (Hendricks, Posnjak & Kracek, 1932). At high temperatures both molecules (ND_4^+ , NO_3^-) are rotating almost freely and the phase transitions with decreasing temperature are associated with a freezing out of the rotational degrees of freedom (Brown & McLaren, 1962). Shinnaka (1959) studied the molecular rotations in the cubic phase. He studied a number of different rotational modes – the term rotation includes both dynamical rotation and statistical disorder. In all the models the nitrate group was thought to preserve its planar equilateral triangle form. In particular, two models of hindered rotation, namely with eight and twelve equivalent orientations, were put forward. The latter model was preferred as a more reliable one as it explained most of the disk-like maxima observed in the diffuse scatterings (Yamamoto & Shinnaka, 1974).

In this work, when we applied Rietveld's profile refinement method to the neutron powder diffraction data, we could not find any difference between Shinnaka's two models. Therefore we applied direct multipole analysis of the nuclear smearing functions (Kurki-Suonio, 1977) to the determination of the molecular orientations. In this way, information was also obtained from the vibrations and bond lengths of both molecules independently.

2. Experimental

Ammonium nitrate was deuterated as highly as possible from 99.6% D_2O . The powder was kept vacuum-sealed in a glass flask. Just before the measurements a sample of 20 g was unloaded in a He-filled glove bag containing P_2O_5 , finely ground, and sealed in an airtight thin-walled vanadium can of diameter 16 mm. Refinement of the room-temperature data confirmed that the deuteration was very successful. Neutron diffraction measurements were made on the powder

diffractometer (*D1A*) at the high-flux reactor in the ILL (Grenoble) using the wavelength of 1.90818 Å. Unfortunately, the furnace was not designed for temperatures below 473 K and therefore we do not know the exact temperature.

D1A consists of a bank of ten ³He high-pressure counters with 6° angular separation (Hewat & Bailey, 1976). In the measurements described here we used the intensities from seven counters merged together, with the counter bank sweeping through 2θ = 0 to 160°. From the observed profile, shown in Fig. 1, two qualitative features can be seen. First, the intensity of the reflections decreases very quickly with 2θ, indicating almost free rotation of the ammonium and nitrate groups. Secondly, there are strong diffuse scattering peaks, e.g. below the (110) reflection, which also are due to the rotations of the molecular groups.

3. Structure of cubic ND₄NO₃ from profile refinement

The space group of the cubic phase is *Pm3m* with the centre of the ammonium group at (000). The nitrogen of the nitrate group lies almost at the body-centre position but according to Shinnaka (1959) it is slightly displaced.

For the starting model to be used in the profile refinement (Rietveld, 1969), we supposed that the four deuterium atoms occupy two sets of crystallographically-equivalent positions of tetrahedral symmetry corresponding to a disorder between energetically equivalent orientations. This is the same arrangement as found e.g. in cubic NH₄Cl (Yelon, Cox & Kortman, 1974). For the nitrate group we used Shinnaka's models with eight and twelve orientations. The corresponding atomic positions are given in Table 1.

In the refinement two sets of parameters were refined; those describing the characteristics of the diffractometer and those describing the crystal structure. The former group consisted of five parameters; the counter zero point, the three half-width parameters and the asymmetry parameter. The structural parameters

refined were the scale factor, the lattice constant, the fractional coordinates – four for the eight-orientations model and five for the twelve-orientations model – and the isotropic thermal vibrational parameters *B* for each atom. The scattering lengths used were *g_N* = 9.4, *g_O* = 5.8, and *g_D* = 6.38 fm (Bacon, 1972).

With the eight-orientations model we could not allow the displacement parameter of nitrogen atom *u*₁ to vary freely because of its high correlation with the oxygen parameters. For similar reasons, in the twelve-orientations model we had to fix *w*₁ and *w*₂ and constrain the values of *v*₃ and *w*₃ so that the angle O–N–O = 120°.

Table 2 gives the values obtained for the displacement parameters and temperature factors. The given reliability factors are calculated from the equation

$$R_{\text{PROF}} = 100 \frac{\sum_i |y_{\text{obs}} - y_{\text{calc}}|}{\sum_i y_{\text{obs}}} \%$$

where *y_i* is the intensity at an angle *θ_i* in the diffraction pattern and the summation is made over all the measured positions *i*. Shinnaka's results were calculated supposing the nitrate group to have a N–O distance of 1.22 Å. From the profile refinement the interatomic distances were, before correcting for thermal libration:

for eight-orientations model:

$$\begin{array}{ll} \text{N–O} & 1.261 (1) \text{ \AA} \\ \text{O–N–O} & 111.0 (7)^\circ \end{array} \quad \begin{array}{ll} \text{N–D} & 0.957 (7) \text{ \AA} \\ \text{D–N–D} & 109.5^\circ; \end{array}$$

for twelve-orientations model:

$$\begin{array}{ll} \text{N–O(1)} & 1.218 \text{ \AA} \\ \text{N–O(2)} & 1.374 (10) \text{ \AA} \\ \text{O–N–O} & 120^\circ. \end{array} \quad \begin{array}{ll} \text{N–D} & 0.994 (5) \text{ \AA} \\ \text{D–N–D} & 109.5^\circ \end{array}$$

Table 1. Coordinates of the atoms in the space group *Pm3m* after Shinnaka's (1959) models

Displacements are denoted by *u*, *v* and *w*.

		Eight orientations of NO ₃ group			Twelve orientations of NO ₃ group				
		<i>x</i>	<i>y</i>	<i>z</i>	<i>x</i>	<i>y</i>	<i>z</i>		
N(1)	8 <i>g</i>	<i>u</i> ₁	<i>u</i> ₁	<i>u</i> ₁	N(1)	6 <i>f</i>	$\frac{1}{2}$	$\frac{1}{2}$	<i>w</i> ₁
O	24 <i>m</i>	<i>u</i> ₂	<i>u</i> ₂	<i>w</i> ₂	O(1)	6 <i>f</i>	$\frac{1}{2}$	$\frac{1}{2}$	<i>w</i> ₂
					O(2)	24 <i>l</i>	$\frac{1}{2}$	<i>v</i> ₃	<i>w</i> ₃
		Tetrahedral coordination of ND ₄ group							
		<i>x</i>	<i>y</i>	<i>z</i>					
N(2)	1 <i>a</i>	0	0	0					
D	8 <i>g</i>	<i>u</i> ₄	<i>u</i> ₄	<i>u</i> ₄					

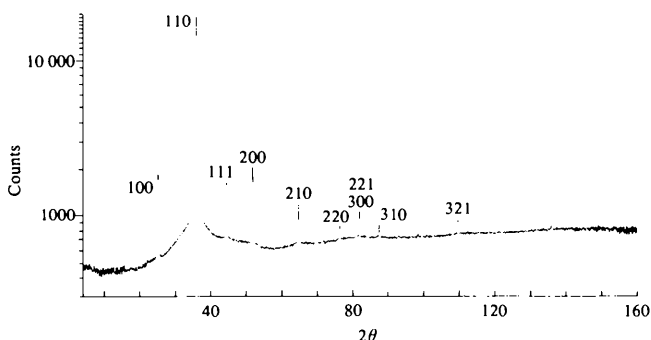


Fig. 1. Neutron powder diffraction pattern of cubic ND₄NO₃ (logarithmic scale).

We also tried to refine both models with the nitrogen of the nitrate group fixed at the body-centre position. In both cases the NO_3 group was then badly distorted from the planar equilateral triangle.

On the basis of the results from the refinements we could not distinguish between the two models. For both models the R values were low and equal, 0.017; the bond lengths and angles were reasonable; and there was no clear difference between the observed and calculated profiles in either case. Fig. 2 shows the observed and calculated profiles; the corresponding structure factors are given in Table 3.

4. Direct multipole analysis of molecular orientational distributions

Once the neutron structure amplitudes G_j of the crystal are known, the analysis of molecular orientations can

Table 2. Displacements u , v and w for the eight- and twelve-orientations models obtained by Shinnaka (1959) and from the profile refinement

Eight-orientations model		Twelve-orientations model	
Shinnaka (1959)			
$u_1 = 0.554$		$w_1 = 0.55$	$w_2 = 0.784$
$u_2 = 0.44$	$w_2 = 0.782$	$v_3 = 0.768$	$w_3 = 0.41$
Profile refinement			
$u_1 = 0.5179$		$w_1 = 0.55$	$w_2 = 0.829$
$u_2 = 0.4570$ (36)	$w_2 = 0.7936$ (17)	$v_3 = 0.7725$ (20)	$w_3 = 0.3925$
$u_4 = 0.1265$ (9)		$u_4 = 0.1248$ (6)	
$B(\text{N1}) = 13.0$ (2) \AA^2		$B(\text{N1}) = 13.0$ (2) \AA^2	
$B(\text{O}) = 13.8$ (5)		$B(\text{O1}) = 11.9$ (8)	
		$B(\text{O2}) = 10.5$ (8)	
$B(\text{N2}) = 13.2$ (3)		$B(\text{N2}) = 11.6$ (2)	
$B(\text{D}) = 14.3$ (3)		$B(\text{D}) = 14.0$ (3)	
$a = 4.3655$ (2) \AA		$a = 4.3655$ (2) \AA	
$R_{\text{PROF}} = 1.7\%$		$R_{\text{PROF}} = 1.7\%$	

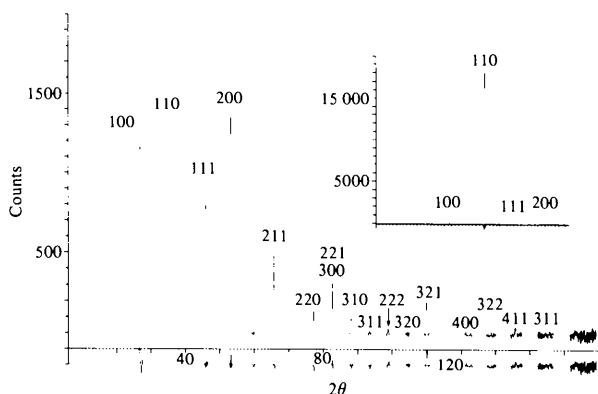


Fig. 2. Observed profile of cubic ND_4NO_3 when the background is subtracted (linear scale). The differences of the observed and calculated values are determined on the basis of the eight-orientations model for NO_3^- .

be based on direct study of the nuclear distributions. Such a method using multipole expansions around the molecular centre has been introduced by Kurki-Suonio, Merisalo, Vahvaselkä & Larsen (1976) and applied to cubic NH_4Cl .

The density function

$$s(\mathbf{r}) = \frac{1}{V} \sum G_j \exp(-2\pi i \mathbf{S}_j \cdot \mathbf{r}), \quad (1)$$

corresponding to the scattering amplitudes G_j , is the weighted sum $\sum g_n \tau_n(\mathbf{r} - \mathbf{r}_n)$ of the statistical nuclear distribution functions $\tau_n(\mathbf{r})$ of all nuclei. The weight g_n is the neutron scattering length of the n th nucleus. In studying molecular orientations it is appropriate to treat it as a sum,

$$s(\mathbf{r}) = \sum s_n(\mathbf{r} - \mathbf{r}_n), \quad (2)$$

of contributions $s_n(\mathbf{r})$ of the molecules rather than of the single nuclei. Thus, in the present case the sum (2) consists of two kinds of distribution functions corresponding to the two molecules. Separated into their nuclear contributions they can be written as

$$s_+(\mathbf{r}) = g_N \tau_{\text{N(1)}}(\mathbf{r}) + 4g_D \tau_D(\mathbf{r}), \quad (3)$$

$$s_-(\mathbf{r}) = g_N \tau_{\text{N(2)}}(\mathbf{r}) + 3g_O \tau_O(\mathbf{r}), \quad (4)$$

where the nuclear distributions have the normalization

$$\int \tau_n(\mathbf{r}) d^3 r = 1.$$

Each molecular contribution $s_n(\mathbf{r})$ and its Fourier transform $\sigma_n(\mathbf{S})$ can be expressed as a site symmetric multipole expansion

$$s_n(\mathbf{r}) = \sum_{lv} s_{lv}^n(r) K_{lv}(\theta, \varphi), \quad (5)$$

$$\sigma_n(\mathbf{S}) = \sum_{lv} \sigma_{lv}^n(S) K_{lv}(\theta_S, \varphi_S), \quad (6)$$

in the spherical coordinates r , θ , φ and S , θ_S , φ_S of real and reciprocal space, respectively (Kurki-Suonio, 1977). In the present case the expansions involve the cubic harmonics $K_{lv}(\theta, \varphi)$.

If the distribution function $s_n(\mathbf{r} - \mathbf{r}_n)$ of the n th molecule is spatially well-separated from those of the neighbouring molecules, the radial distribution $s_{lv}^n(r)$ is readily obtained by expanding the Fourier series (1) as a multipole expansion around r_n . This yields

$$s_{lv}^n(r) = \frac{4\pi(-i)^l}{VA_{lv}} \sum_j G_j \exp(-2\pi i \mathbf{S}_j \cdot \mathbf{r}_n) j_l(2\pi S_j r) \times K_{lv}(\theta_j, \varphi_j), \quad (7)$$

where $j_l(x)$ is the spherical Bessel function of order l , $A_{lv} = \int K_{lv}^2 d\Omega$, and S_j , θ_j , φ_j are the spherical coordinates of the j th reciprocal-lattice vector. If all the molecular distributions $s_n(\mathbf{r})$ and no contribution from

the neighbours lie within a radius R_n , this expression for $r \leq R_n$ gives a true representation of $s_n(r)$ in form of the site symmetric multipole expansion (5).

The molecular radial scattering amplitude $\sigma_{lv}^n(S)$ is the l th-order Fourier–Bessel transform of $s_{lv}^n(r)$. It is, thus, obtained from (7) through

$$\begin{aligned} \sigma_{lv}^n(S) &= 4\pi i^l \int_0^{R_n} s_{lv}^n(r) j_l(2\pi Sr) r^2 dr \\ &= \frac{16\pi^2 R_n^3}{VA_{lv}} \sum_j G_j \exp(-2\pi i \mathbf{S}_j \cdot \mathbf{r}_n) \\ &\quad \times \frac{x_j j_{l+1}(x_j) j_l(x_j) - x_j j_{l+1}(x_j) j_l(x_j)}{x^2 - x_j^2} K_{lv}(\theta_j, \varphi_j), \quad (8) \end{aligned}$$

where $x = 2\pi R_n S = 4\pi R_n \sin \theta / \lambda$ and $x_j = 2\pi R_n S_j$.

The series (7) and (8) give the possibility of calculating the radial distributions $s_{lv}^n(r)$ and scattering amplitudes $\sigma_{lv}^n(S)$ for each molecule separately, directly from the experimental structure amplitudes G_j . In the case of large thermal amplitudes, the multipole expansions (5), (6) converge rapidly and yield a simple description of the nuclear distributions. Moreover, in case of rigid molecules this description of the thermal motion in spherical coordinates around the molecular centre is much more appropriate than a representation

in terms of vibrations of the single atoms around their equilibrium positions.

For the present study the experimental structure amplitudes G_j were taken from the results of the preceding profile refinements (Table 3). The refinement is understood to put them on an absolute scale, to make all necessary corrections and to define their correct signs. This is naturally model dependent. Therefore, the analysis was made with both sets of experimental G_j obtained using the two Shinnaka models. All differences in the results were, however, an order of magnitude smaller than the direct experimental uncertainties and not visible in the scale of figures representing the results.

As the reference model for difference series calculations, we took a crystal composed of freely-rotating rigid ND₄⁺ and NO₃⁻ groups in their ideal positions with N–D and N–O bond lengths r_{01} and r_{02} and in harmonic vibration corresponding to the Debye–Waller factors B_+ and B_- , respectively. The model structure amplitudes are, thus,

$$G_j = \sigma_+(\mathbf{S}_j) + \sigma_-(\mathbf{S}_j) \exp[\pi i(h+k+l)], \quad (9)$$

with

$$\sigma_0^+(\mathbf{S}) = [g_N + 4g_{\text{D}j_0}(2\pi r_{01} S)] \exp(-B_+ S^2/4), \quad (10)$$

$$\sigma_0^-(\mathbf{S}) = [g_N + 3g_{\text{O}j_0}(2\pi r_{02} S)] \exp(-B_- S^2/4). \quad (11)$$

Table 3. *Compilation of the structure factors*

The experimental structure factors, G_{obs} (12), and those calculated on the basis of Rietveld profile-refinement method, $G_{\text{calc}}(RM)$, have the signs and splitting of the overlapping reflections determined according to the twelve-orientations model. $G_{\text{calc}}(0)$ are calculated from the zeroth-order components of the radial scattering amplitudes from (10) and (11); in $G_{\text{calc}}(4)$ the fourth-order components are also taken into account.

hkl	$G_{\text{obs}}(12)$	$G_{\text{calc}}(RM)$	$G_{\text{calc}}(0)$	$G_{\text{calc}}(4)$
1 0 0	0.71593	0.69868	0.75444	0.67233
1 1 0	2.39417	2.38848	2.47109	2.44635
1 1 1	0.78067	0.77842	0.44829	0.71319
2 0 0	1.17666	1.16546	1.00870	1.17939
2 1 0	0.01160	0.08728	0.18926	0.07113
2 1 1	0.40730	0.41456	0.46309	0.42594
2 2 0	0.32624	0.35464	0.26963	0.24957
3 0 0	-0.60334	-0.60049	-0.02254	-0.55314
2 2 1	0.18530	0.18443	-0.02254	0.23293
3 1 0	0.22715	0.25078	0.19921	0.20511
3 1 1	-0.08299	-0.14674	-0.02822	-0.11863
2 2 2	0.18394	0.14774	0.16574	0.19150
3 2 0	-0.04526	0.03026	-0.01583	0.00403
3 2 1	0.21203	0.17573	0.14092	0.15691
4 0 0	0	0.05425	0.11504	0.04722
4 1 0	0	0.10881	0.01197	-0.08588
3 2 2	0	0.00999	0.01197	0.08267
3 3 0	0.21494	0.16262	0.09518	0.11134
4 1 1	0.06205	0.04696	0.09518	0.06347
3 3 1	0.04700	0.00659	0.01886	0.04992
R%		5.7	26.5	8.9

On the basis of the preceding powder-profile refinements, the model parameters were given the values $r_{01} = 0.96$, $r_{02} = 1.26$ Å, and $B_+ = B_- = 13.0$ Å².

In terms of the multipole expansions (5), (6), both molecules in the model contain just the spherical or zeroth-order component. A difference series calculation of series (8) in the zeroth order will yield deviations $\Delta\sigma_0^+$ and $\Delta\sigma_0^-$ from the model, which could be due to erroneous values of the bond lengths, or of the Debye–Waller factors, or to non-rigidity of the molecule, or to anharmonicity of its positional distribution. In the higher orders we just get the experimental estimates for σ_{lv}^+ and σ_{lv}^- which represent the deviations of the molecular distribution function from sphericity and will, thus, show the nature of the librational motion. The radius R_n in (8) was taken as half the distance of neighbouring ions, or $R_+ = R_- = 1.90$ Å. The resulting radial scattering amplitudes $\Delta\sigma_{lv}^+$ and $\Delta\sigma_{lv}^-$ are shown in Fig. 3 with error bars referring to the statistical errors of the experimental G_j .

5. Discussion and conclusions

It is obvious from the results that the experimental data indicate significant deviations from the spherical-ion model only in the fourth-order multipole component.

The molecular scattering amplitudes can thus be represented as

$$\sigma_{\pm}(\mathbf{S}) = \sigma_0^{\pm}(S) + \sigma_4^{\pm}(S)K_4(\theta_S, \varphi_S), \quad (12)$$

where σ_0^+ and σ_0^- are given by the spherical model values (10) and (11), respectively, and $\sigma_4^+(S)$ and $\sigma_4^-(S)$ are given by the corresponding curves in Fig. 3.

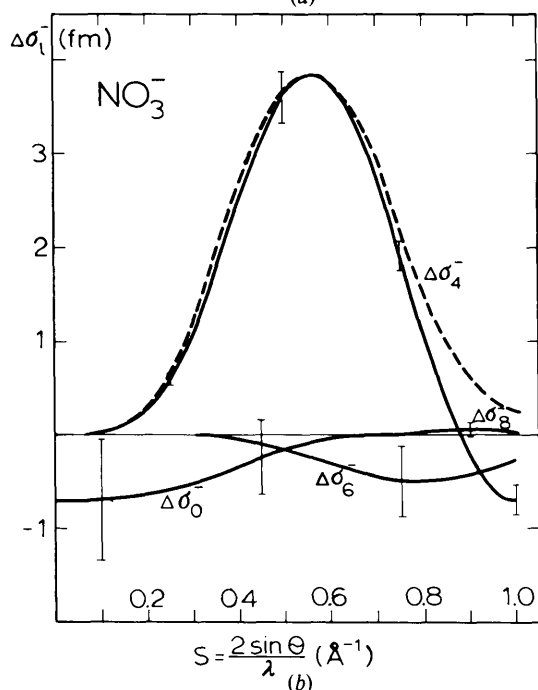
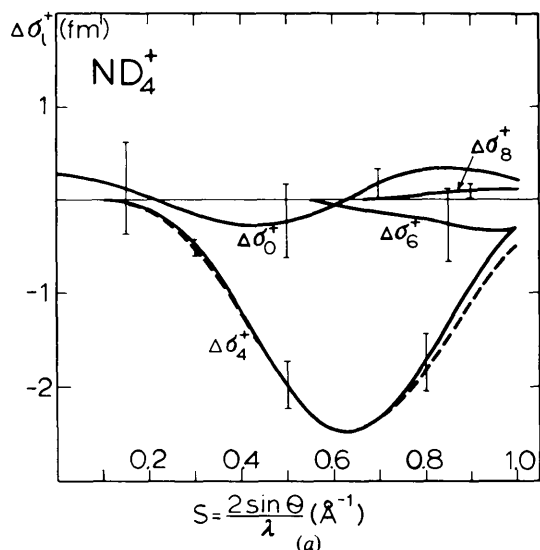


Fig. 3. Radial scattering amplitudes $\Delta\sigma_l^{\pm}$ for (a) ND_4^+ and (b) NO_3^- . The experimental values (solid line) are calculated from (8) using (10) and (11) as reference models. The error bars refer to the statistical errors of the experimental structure factors G_j . The theoretical curves (broken line) are calculated from the model (16) with the parameters of Table 4.

Since σ_4^+ is negative, the orientational distribution of the deuterons in ND_4^+ has the nature of $-K_4(\theta, \varphi)$, with maxima in the [111] and symmetry-related directions and minima in the [100] and related directions. This confirms the known dominance of the two symmetry-related tetrahedral orientations of ND_4^+ . σ_4^- is positive; therefore the orientational distribution of the oxygens in NO_3^- has maxima in [100] and minima in [111] and related directions, such as $K_4(\theta, \varphi)$. This gives clear preference of the orientations in the 12-orientations model over those of the eight-orientations model.

A more detailed interpretation of the results becomes possible through a closer study of the multipole expansions (5), (6), corresponding to rigid molecules. In a non-vibrating molecule, N similar nuclei (with the scattering length g) at the distance of a given bond length r_0 from the centre of the molecule yield a density contribution

$$s(\mathbf{r}) = Ng \frac{\delta(r - r_0)}{4\pi r^2} f(\theta, \varphi). \quad (13)$$

Here $f(\theta, \varphi)$ is the angular distribution of the nuclei around the centre normalized to $\int f(\theta, \varphi) d\Omega = 4\pi$. It can be written in the form of a site symmetric multipole expansion

$$f(\theta, \varphi) = 1 + \sum_{l>0} c_{lv} K_{lv}(\theta, \varphi), \quad (14)$$

where

$$c_{lv} = \frac{\int K_{lv}(\theta, \varphi) f(\theta, \varphi) d\Omega}{\int [K_{lv}(\theta, \varphi)]^2 d\Omega}. \quad (15)$$

The corresponding expansion for the molecular scattering amplitude is the Fourier transform of (13) or

$$\sigma(\mathbf{S}) = Ng [j_0(2\pi S r_0) + \sum_{l>0} i^l c_{lv} j_l(2\pi S r_0) K_{lv}(\theta_S, \varphi_S)]. \quad (16)$$

If we allow for harmonic vibrations of the molecule this contribution should just be multiplied by the corresponding Debye-Waller factor.

Interpretation of the experimental curves for σ_{lv}^n presented in Fig. 3 involves in the first place comparison with a model composed of rigid molecules in harmonic vibration and with an orientational distribution independent of the vibrations. For the spherical component this brings us back to (10) and (11); for the non-spherical ones we have, according to (16),

$$\sigma_{lv}^+(\mathbf{S}) = 4g_D i^l c_{lv} j_l(2\pi S r_{01}) \exp(-B_+ S^2/4), \quad (17)$$

$$\sigma_{lv}^-(\mathbf{S}) = 3g_O i^l c_{lv} j_l(2\pi S r_{02}) \exp(-B_- S^2/4). \quad (18)$$

Comparison of the experimental curves (Fig. 3) with these model curves shows a very good fit in the general behaviour. The spherical components give information on the bond lengths and Debye-Waller factors independently of the orientational behaviour. After slight

adjustments of B_+ and B_- we find that the positions of the maxima in both σ_0 and σ_4 indicate consistently small changes of the bond lengths. Then c_4^+ and c_4^- are adjusted to produce the final fit of the model to the experimental curves. The resulting parameters are listed in Table 4 and the corresponding model curves are shown in Fig. 3. We conclude that the experimental data do not indicate any significant deviations from our model.

In Table 3 the structure factors calculated in different ways are compared. The reliability index, defined by

$$R = \frac{\sum |G_{\text{obs}}| - |G_{\text{calc}}|}{\sum |G_{\text{obs}}|} \times 100\%$$

shows a large drop from 26.5 to 8.9% when the fourth-order components of the radial scattering amplitudes are taken into account. This shows that the two parameters c_4 represent very well the deviations from the spherical model. When compared with 5.7% obtained from the profile refinement one has to note that this value is reached by a simultaneous refinement of a total of thirteen parameters and ours is a result of just a direct calculation of two parameters independently of each other and of any other parameter. A refinement of our parameters, together with the Debye-Waller factors and bond lengths and with the necessary external parameters, is obviously possible and would yield a better fit. The program used for the powder profile refinement did not, however, allow immediate application of this model.

Table 4. Values of parameters in cubic ND₄NO₃ from the multipole analysis

ND ₄ ⁺	NO ₃ ⁻
$B_+ = 11.5 (1) \text{ \AA}^2$	$B_- = 14.3 (1) \text{ \AA}^2$
$r_{\text{N-D}} = 0.99 (1) \text{ \AA}$	$r_{\text{N-O}} = 1.23 (1) \text{ \AA}$
$c_4^+ = -2.6 (5)$	$c_4^- = 4.4 (5)$
$c_6^+ = +1 \pm 2$	$c_6^- = +2 \pm 2$
$c_8^+ = 0.2 \pm 0.2$	$c_8^- = -0.3 \pm 0.3$

Table 5. Values of the multipolar coefficients c_{lv} for different non-librating molecular orientation models

Model	c_4	c_6	c_8
ND ₄ ⁺			
Tetrahedral group	-3.5	5.1	2.6
Tetrahedral group with rotations around N-D	-0.8	2.0	-1.1
NO ₃ ⁻			
Twelve orientations	2.0	-0.9	5.1
Twelve orientations with rotations around N-O	0.7	2.1	2.5
Eight orientations	-1.3	1.5	-3.5

The parameters c_{lv}^{\pm} obtained give already a complete description of the orientational distribution of the molecules as indicated by the data. Absence of all higher than fourth-order moments indicates strong librational motion, which cannot be well approximated by any model based on fixed atomic positions. To make the result more concrete we list in Table 5 for comparison the multipolar coefficients for some specific orientational models. The relevant principles of calculation are presented in the Appendix.

Interpretation of the experimental values of c_{lv} in terms of a rigid molecule librating around a fixed orientation requires that the ratios $c_{lv}^{\text{obs}}/c_{lv}^{\text{model}}$ can be identified with the libration factors a_l in (A9), (A10). Thus, they have to be positive and < 1 and, moreover, fulfil (A11).

For ND₄, c_4^{obs} is obviously consistent with the normal tetrahedral coordination giving $a_4 = 0.74$. According to (A11) this corresponds to the r.m.s. angular amplitude $\beta = 9.2^\circ$, or $\langle u_L^2 \rangle^{1/2} = r_{\text{N-D}} \beta = 0.16 \text{ \AA}$ for the libration. Further, this amplitude would give $a_6 = 0.46$, $a_8 = 0.07$, $c_6 = 2.3$ and $c_8 = 0.2$ which within the error limits agree with the insignificance of the corresponding experimental values.

As to NO₃, the experimental value $c_4 = 4.4$ is much too large to be explained by any fixed-orientation model of a rigid NO₃. Shinnaka's twelve-orientations model gives the maximum possible value of c_4 for such models. This is still less than half of the experimental value. From the behaviour of K_4 it is obvious that only a high concentration of the oxygens at the octahedral orientations $\langle 100 \rangle$ makes such a high value of c_4 possible. A complete octahedral coordination would correspond to $c_4 = 5.25$. This, however, is impossible for a rigid NO₃, particularly as the observed distance, 1.23 Å, of the oxygens from the centre corresponds well with the normal bond length of NO₃. We could not find any indication of the nitrogen atoms having orientational distribution around their central position.

APPENDIX

Calculation of multipolar coefficients c_{lv} for some molecular orientational models

The angular distribution function $f(\theta, \varphi)$ of N similar nuclei at a distance r_0 from the molecular centre is defined by (13). For any given orientational model, the calculation of multipolar coefficients c_{lv} in (14) is in principle straightforward through (15) since $f(\theta, \varphi)$ is a known function. We can always write

$$f(\theta, \varphi) = \hat{S} \left[\frac{1}{N} \sum_{i=1}^N f_i(\theta, \varphi) \right], \quad (\text{A1})$$

where $f_i(\theta, \varphi)$ is the angular distribution of the i th atom in one of the possible symmetry-equivalent orienta-

tions of the molecule and S means site symmetrization (*i.e.* averaging over all symmetry-equivalent orientations). Substitution in (15) yields immediately the coefficients as a sum of contributions from the individual atoms

$$c_{lv} = \sum_{i=1}^N c_{lv}^i = \frac{1}{N} \frac{\sum_{i=1}^N \int K_{lv}(\theta, \varphi) f_i(\theta, \varphi) d\Omega}{\int K_{lv}^2 d\Omega}. \quad (A2)$$

The symmetrization is automatically taken into account by the symmetry of the harmonics K_{lv} .

(a) Fixed orientation

If the i th atom in its basic position has a fixed orientation in the direction θ_i, φ_i , then

$$f_i(\theta, \varphi) = 4\pi \frac{\delta(\theta - \theta_i)}{\sin \theta} \delta(\varphi - \varphi_i), \quad (A3)$$

and

$$c_{lv}^i = \frac{(4\pi/N)K_{lv}(\theta_i, \varphi_i)}{\int K_{lv}^2 d\Omega}. \quad (A4)$$

(b) Rotation about a fixed axis

If the molecule in its basic orientation is in free rotation about an axis in the direction θ_0, φ_0 through the molecular centre, then

$$f_i(\theta, \varphi) = 2 \frac{\delta(\theta' - \alpha_i)}{\sin \theta'}, \quad (A5)$$

where θ' is the polar angle with respect to the rotation axis and α_i is the value of this angle for the i th atom. We then have

$$c_{lv}^i = \frac{(4\pi/N)K_{lv}(\theta_0, \varphi_0)P_l(\cos \alpha_i)}{\int K_{lv}^2 d\Omega}. \quad (A6)$$

(c) Isotropic Gaussian libration

If, in the basic orientation of the molecule, the i th atom is performing small harmonic librations about its equilibrium orientation, θ_i, φ_i isotropically in all angular directions, we can make use of the distribution

$$f_i(\theta, \varphi) = \frac{2}{\beta^2(1-\varepsilon)} \exp(-\theta'^2/2\beta^2) \frac{\theta'}{\sin \theta'}, \quad (A7)$$

where $\varepsilon = \exp(-\pi^2/2\beta^2)$ and θ' is the angle measured from the direction θ_i, φ_i . For this distribution the r.m.s. angular amplitude is

$$\langle \theta'^2 \rangle = 2\beta^2 \left(1 - \frac{\pi^2}{2\beta^2} \frac{\varepsilon}{1-\varepsilon} \right). \quad (A8)$$

In the limit $\beta \ll \pi$ it is a Gaussian distribution with $\langle \theta'^2 \rangle = 2\beta^2$. This yields, for the multipolar coefficient,

$$c_{lv}^i = \left(\frac{4\pi}{N} \right) \frac{K_{lv}(\theta_i, \varphi_i)}{\int K_{lv}^2 d\Omega} a_l(\beta), \quad (A9)$$

$$a_l(\beta) = \frac{1}{\beta^2(1-\varepsilon)_0} \int_0^\pi \exp(-\theta'^2/2\beta^2) \theta P_l(\cos \theta) d\theta. \quad (A10)$$

This differs from the corresponding expression (A4) for the non-librating case by the factor a_l .

If, in the integral, $P_l(\cos \theta)$ is replaced by its maximum value one this factor becomes one. This shows that such a libration always reduces the absolute value of c_{lv}^i . Further, if all atoms of the group librate similarly with the same angular amplitude, the coefficient c_{lv} of the whole group is reduced by the same factor $a_l(\beta)$ which thus can be called the l th-order libration factor.

For small amplitudes ($\beta \ll \pi$) only small values of θ contribute to the integral in (A10) and we can approximate

$$P_l(\cos \theta) \simeq P_l(1) - \frac{1}{2} P_l'(1) \theta^2 = 1 - l(l+1) \theta^2/4.$$

This yields for the libration factor the estimate

$$a_l \simeq 1 - [l(l+1)/2] \beta^2. \quad (A11)$$

This result shows quite generally that small isotropic librations reduce the l th multipole components of a molecular distribution function or scattering amplitude by a libration factor a_l given by (A11). The libration factor a_l is independent of the geometry of the molecule, of its orientation and of the site symmetry. It decreases with increasing librational amplitude and with increasing multipolar order l .

The help of Dr K. Österlund in preparing the deuterated ammonium nitrate is gratefully acknowledged. We would also like to thank the ILL for all facilities.

References

- BACON, G. E. (1972). *Acta Cryst.* **A28**, 357–358.
 BROWN, R. N. & MCLAREN, A. C. (1962). *Proc. R. Soc. London*, **266**, 329–343.
 CHOI, C. S., MAPES, J. E. & PRINCE, E. (1972). *Acta Cryst.* **B28**, 1357–1361.
 HENDRICKS, S. B., POSNJAK, E. & KRACEK, F. C. (1932). *J. Am. Chem. Soc.* **54**, 2766–2786.
 HEWAT, A. W. & BAILEY, I. (1976). *Nucl. Instrum. Methods*, **137**, 463–471.
 KURKI-SUONIO, K. (1977). *Isr. J. Chem.* **16**, 113–123, 132–136.
 KURKI-SUONIO, K., MERISALO, M., VAHVASELKÄ, A. & LARSEN, F. K. (1976). *Acta Cryst.* **A32**, 110–115.
 RIETVELD, H. M. (1969). *J. Appl. Cryst.* **2**, 65–71.
 SHINNAKA, Y. (1959). *J. Phys. Soc. Jpn*, **14**, 1073–1083.
 YAMAMOTO, S. & SHINNAKA, Y. (1974). *J. Phys. Soc. Jpn*, **37**, 724–732.
 YELON, W. B., COX, D. E. & KORTMAN, P. J. (1974). *Phys. Rev. B*, **9**, 4843–4856.